J Mol Model (2011) 17:971–978
DOI 10.1007/s00894-010-0795-4

ORIGINAL PAPER

Molecular modeling and dynamics simulation of a histidine-tagged cytochrome b_5

Ying-Wu Lin · Tian-Lei Ying · Li-Fu Liao

Received: 12 October 2009 / Accepted: 25 June 2010 / Published online: 11 July 2010

Abstract Although an affinity tag such as six consecutive histidines, $(His)_6$-tag, has been widely used to obtain high quantity of recombinant proteins, little is known about its influences on heme proteins for lack of structural information. When $(His)_6$-tag was introduced to the N-terminus of a small heme protein, cytochrome b_5, experimental results showed the resultant protein, $(His)_6$-cyt b_5, has similar property and function to that of isolated cyt b_5. To provide structural information for this observation, we herein performed a structural prediction of $(His)_6$-cyt b_5 by molecular modeling in combination with molecular dynamics simulation. The predicted structure, as assessed by a series of criteria with good quality, reveals that the $(His)_6$-tag adopts a helical conformation and packs against the hydrophobic core 2 of cyt b_5 through salt bridges, hydrogen bonding and hydrophobic interactions. The heme group, with the axial His ligands slightly rotated, was found to have similar conformation as in isolated cyt b_5, which indicates that the N-terminal $(His)_6$-tag does not alter the heme active site, resulting in similar dynamics properties for core 1. This study provides valuable information of interactions between $(His)_6$-tag and the rest of the protein, aiding in rational design and application of functional His-tagged proteins.

Keywords Affinity tag · Heme proteins · Hydrogen bonding · Hydrophobic interactions

Y.-W. Lin (✉) · L.-F. Liao
School of Chemistry and Chemical Engineering,
University of South China,
Hengyang 421001, People's Republic of China
e-mail: linlinying@hotmail.com

Y.-W. Lin
Department of Chemistry,
University of Illinois at Urbana-Champaign,
Urbana, IL 61801, USA

T.-L. Ying
Chemical Biology Lab, Department of Chemistry,
Fudan University,
Shanghai 200433, People's Republic of China

Introduction

Histidine tag such as six consecutive histidines, $(His)_6$-tag, has been popularly used for protein purification over the last two decades [1]. It was generally introduced into the N- or C-terminus of a protein of interest to facilitate the purification on a nickel affinity column. Although the tag may be removed by a protease, the cleavage often takes many hours and may considerably impair the target protein by side reactions [2]. Thus, small $(His)_6$-tag is often left on the protein, which however raises a question about its effects on the protein structure and function. Recently, by surveying the crystal structures with and without His-tags within the PDB bank, Carson *et al.* showed that His-tags generally have no significant effects on the structure of the native protein [3]. However, one recent study showed by NMR that an N-terminal G $(H)_6$LE-tag interacts transiently with the rest of the protein Robl1_mouse in solution [4].

Comparatively, in solution little structural information is available from literature about the effects of His-tag on a protein. This is due to the fact that in most cases the $(His)_6$-tag is too mobile to provide NOR constraints in NMR structure determination. On the other hands, as a complement to experiments, molecular dynamics (MD) simulation offers a valuable approach to provide an atomic level as well as a time-dependent view of protein structure

in solution [5]. Therefore, it is possible to investigate the effects of His-tag on the structure of a given protein by means of MD simulation. As shown recently by Freydank *et al.* from a relative short MD simulation (100 ps, 300 K), the $(His)_6$-tag attached at the C-terminus of tropinone reductase can interfere with the enzyme active site by steric or electrostatic interactions [6].

In a previous study, in order to simplify the purification procedure of cytochrome b_5 (cyt b_5), a small heme protein with heme bound non-covalently by two axial histidine ligands (His39 or His63), we expressed it as a glutathione S-transferase (GST) fusion protein, GST-cyt b_5, and purified it on a one-step affinity column chromatography with glutathione-agarose gel [7]. Alternatively, we cloned the cyt b_5 gene into an expression vector of pQE-30 that attached a $(His)_6$-tag to the N-terminus of cyt b_5, $(His)_6$-cyt b_5, which was then purified by a one-step nickel affinity column [8]. Also, other researchers used this method for cyt b_5 purification [9, 10]. Both $(His)_6$-cyt b_5 and GST-cyt b_5 expression systems have their advantages in comparison to conventional system such as pUC19 or pET11, particularly when they aim to obtain cyt b_5 mutants with altered axial ligands, e.g., H39S or H39C [11], since these mutants were matured as apoproteins with no heme group incorporated due to the loss of one of the two axial His ligands. The one-step purification process thus overcomes the drawbacks of the colorless apocyt b_5 that has low stability in the absence of heme group.

Although we have shown that the GST protein fused to the N-terminus of cyt b_5 has no significant effects on the structure and function of cyt b_5 [7], we know little about the structural information of $(His)_6$-tag, since it is comparatively small and more flexible. Previous study [9] as well as our preliminary investigations [8] showed that it has slight to no impact on cyt b_5. However, we are short of the structural information of $(His)_6$-cyt b_5 to support the experimental observations, even though isolated cyt b_5 was well-studied [12, 13]. Actually, to the best of our knowledge, in the case of heme proteins few efforts have been attempted to investigate the effects of His-tag on the protein structure and function to date. However, this issue is important for heme proteins since the His-tag might have a chance to interact with the heme group or the substrate directly or indirectly, and thus exerts influences on protein functions. In a very recent study, by enzyme assay and docking simulation Yamazaki *et al.* showed that substrate midazolam could not easily access the heme center of histidine-tagged cytochrome P450 3A5, with high interaction energy compared with isolated P450 3A5, resulting in no detectable activities of midazolam hydroxylation [14]. Meanwhile, the detail interactions of His-tag with the polypeptide chain of P450 3A5 were not well defined. With these in mind, we herein performed molecular modeling in combination with MD simulations for $(His)_6$-cyt b_5, aimed at providing structural information at atomic level about the influence of His-tag on the structure and function of heme proteins in solution. Additionally, modeling of $(His)_6$-cyt b_5 will guide future studies such as self-assembly of $(His)_6$-cyt b_5 based on the affinity tag, providing deeper insights into native cyt b_5 system.

Materials and methods

System setup

As expressed in pQE-30, $(His)_6$-cyt b_5 has a peptide of MRGSHHHHHHG attached at its N-terminus [8]. According to this sequence, the initial structure of $(His)_6$-cyt b_5 was constructed by combination of the conformation of cyt b_5 obtained from NMR structure (PDB entry 1hko [12], model 1, a fragment of Ser5-Ser97 corresponding to lipase proteolysis with 93 residues was selected) and the His-tag generated by Swiss-PdbViewer 4.0.1. [15], a program used previously for construction of a His-tagged cytochrome *c* oxidase model [16]. It should be noted that the His-tag was constructed as a short α-helix by this program. As a result, the constructed $(His)_6$-cyt b_5 contains 104 amino acids (Met1-Ser104). The psfgen of program NAMD 2.7 b1 (Nanoscale Molecular Dynamics) [17] was used to add hydrogen atoms and assign charges to the protein, which is set up according to pH 7. Note that according to experimental observations in physiological pH range (~7.4), the δ-nitrogen of histidine was protonated for $(His)_6$-cyt b_5. The protein was then solvated in a cubic box (about 85 Å × 65 Å × 60 Å) of TIP3 water with periodic boundary conditions, which extended 15 Å away from any given protein atom. The $(His)_6$-cyt b_5 water system was then neutralized by adding a total of 28 counter ions (17 Na^+ and 11 Cl^-) by using the autoionize plug-in of program VMD 1.8.7 (Visual Molecular Dynamics) [18], resulting in the physiological ionic strength of 0.15 M.

Minimization and MD simulation protocols

To search the conformation of His-tag in $(His)_6$-cyt b_5, a minimization protocol was performed as described previously [19]. Shortly, the system was minimized 1,000 steps, followed by a MD simulation with the temperature gradually drop from 550 to 300 K (increment: −50 K, with equilibration for 200 ps at each temperature and the step size is 1 fs), and then were reminimized for 50,000 steps. The non-bonded interaction cutoff distance was set to be 9 Å. In the first cycle of minimization, residues

Val15-Ser104 of $(His)_6$-cyt b_5 were fixed, while the N-terminal residues of Met1-Ala14 containing the His-tag, as well as the counter ions and water molecules, were allowed to move. In the second cycle of minimization, only residues from His26 (at the end of α1) to Ile86 (at the end of α5) were fixed in $(His)_6$-cyt b_5, while both N-terminal residues including His-tag, α1 and β1 (Met1-Lys25) and C-terminal residues including β2 and α6 (Ile87-Ser104) were allowed to move. For further model refinement, the resulting $(His)_6$-cyt b_5 system was subjected to two MD simulations with temperature hold at 300 K for 2 ns. A control MD simulation on isolated cyt b_5 (Ser12-Ser104) without the $(His)_6$-tag was also performed under identical conditions. Coordinates were saved every 1,000 steps (corresponding to 2 ps) to produce trajectory files containing 1,000 configurations for each 2-ns of simulation. The simulations were carried out with the program NAMD 2.7 b1. Visualization and data analysis were done with VMD 1.8.7.

Criteria to assess the modeling structure

A series of criteria were used to assess the modeling structure of $(His)_6$-cyt b_5: (i) The modeling structure was evaluated by ProSA (Protein Structure Analysis) as accessible at https://prosa.services.came.sbg.ac.at. It is an established tool that has a large user base and is frequently employed in the refinement and validation of experimental protein structures and in structure prediction and modeling [20]; (ii) The modeling structure was overlapped with the initial NMR structure of cyt b_5 as well as the MD simulation result of cyt b_5, and Ramachandran plot analysis was further performed for these structures by using VMD 1.8.7; (iii) The dynamic property of $(His)_6$-cyt b_5 was compared to that of isolated cyt b_5 in this study and previous MD simulations of cyt b_5 [21–23] and apocyt b_5 [24–27]; (iv) The $(His)_6$-tag conformation and its intramolecular interactions with $(His)_6$-cyt b_5 were compared to several crystal structures from PDB bank with $(His)_6$-tag being well determined; (v) The structure of $(His)_6$-cyt b_5 including both core 1 (heme-binding domain) and core 2 was compared to the initial NMR structure as well as the crystal structure of cyt b_5 (PDB entry 1cyo [12]); (vi) And the effects of $(His)_6$-tag on the property of cyt b_5 was evaluated by comparison to the experimental results of our recent study [8].

Results and discussion

Modeling structure of $(His)_6$-cyt b_5

With two cycles of energy minimization, followed by two separated MD simulations, the refined two modeling structures of $(His)_6$-cyt b_5 are shown in Fig. 1. The $(His)_6$-tag keeps most of the helix structure in both cases and packs against core 2 by interacting with α1, α6 and β1 (see next section for details). Although $(His)_6$-tag often adopts an extending conformation as shown in some protein structures with His-tag being well determined [3], it does show a well-folded helical structure in some cases such as in PDB 1w3o [28] and 1v30 [29], depending on the local environments. The rest of protein $(His)_6$-cyt b_5 overlaps well with the initial NMR structure of cyt b_5 as well as the control MD simulation structure of cyt b_5, which indicates that the $(His)_6$-tag introduced at N-terminus of cyt b_5 does not disturb the overall structure in a significant manner. It is interesting to observe that the loop connecting α1 and β1 adopted an open conformation in present simulations. Previous studies also showed that an open-close cleft transition occurred in this region [21–23].

ProSA analysis was performed to check the quality of the modeling structures from minimization and MD simulation. As shown in Table 1, the combined energy z-score decreases from −6.28 of the initial $(His)_6$-cyt b_5 structure to about −6.6 after model refinement by MD simulation, suggesting that a comparatively stable state was achieved. Control experiment of cyt b_5 also shows a slight decrease compared to the initial NMR structure.

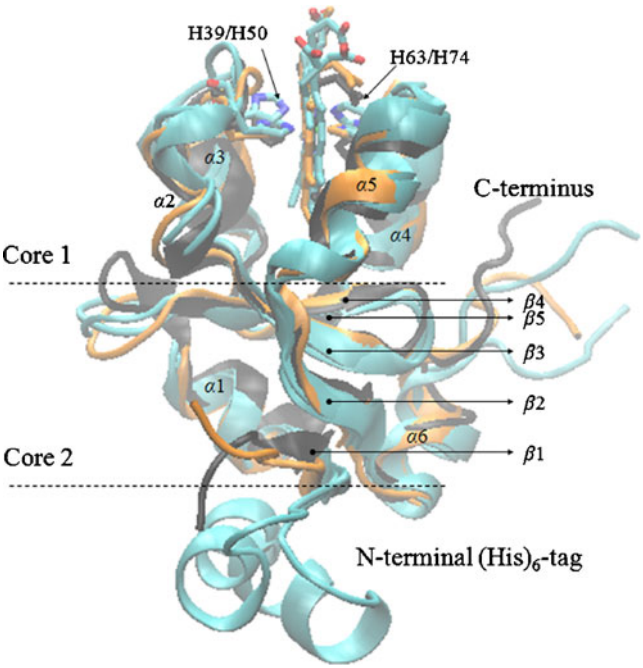

Fig. 1 The overlapping view of two modeling structures of $(His)_6$-cyt b_5 (cyan) with the initial NMR structure of cyt b_5 (PDB entry 1hko, model 1, black) and that after MD simulation (orange). The two distinct regions, core 1 and core 2 (separated by dashed line), the heme group with two axial ligands (His39 or His50 and His63 or His74), the elements of secondary structure, helix α1-6, five β strands (β1-5) (indicated by arrows), as well as the N-terminal $(His)_6$-tag and C-terminus are highlighted

Table 1 Calculated z-score values for the initial and modeling structure of cyt b_5 and $(His)_6$-cyt b_5 by program ProSA

Structure	z-score value
Cyt b_5 (NMR, PDB entry 1hko, model 1) [a]	−7.01
Cyt b_5 (MD simulation)	−7.18
$(His)_6$-cyt b_5 (Initial structure) [b]	−6.28
$(His)_6$-cyt b_5 (Minimization)	−6.44
$(His)_6$-cyt b_5 (MD simulation-1)	−6.58
$(His)_6$-cyt b_5 (MD simulation-2)	−6.63

[a] 93 amino acids (Ser5-Ser97)

[b] 104 amino acids (Met1-Ser104)

Additionally, Ramachandran plots show that over 90% residues are in favored region and allowed region for two models of $(His)_6$-cyt b_5, reflecting the good stereo chemical features. These observations further elucidate the acceptability of the predicted structures of $(His)_6$-cyt b_5.

Furthermore, the total energy of $(His)_6$-cyt b_5 in MD simulations as a function of time step was plotted in Fig. 2a, with that of cyt b_5 shown for comparison. The total energy fluctuates around -65600 kcal mol^{-1} for cyt b_5 and around -45600 kcal mol^{-1} for $(His)_6$-cyt b_5 in both MD simulations during the last 1-ns, suggesting an energy favorable state was achieved. An analysis of the backbone C_α root mean square deviations (RMSD) was further performed for both core 1 and core 2 in $(His)_6$-cyt b_5, and in cyt b_5 as well, with the C-terminal six residues (Thr99-Ser104) excluded (Fig. 2b–d). It can be observed that RMSD fluctuates during the last 0.5-ns MD simulation, indicating an achievement of stable conformation equilibration. The RMSD value of core 1 in both $(His)_6$-cyt b_5 and cyt b_5 is found to be around 1.5 Å, which suggests that the introduction of a $(His)_6$-tag at the N-terminus of cyt b_5 leaves the heme-binding core 1 largely intact. Meanwhile, a slightly lower RMSD value is observed for core 2 in $(His)_6$-cyt b_5 (around 0.75 Å) compared to that in isolated cyt b_5 (around 1.0 Å), indicating that $(His)_6$-tag stabilizes some residues in core 2 to some extent by direct interactions. The different RMSD value between core 1 and core 2 also agrees well with previous MD study of cyt b_5 [21]. Moreover, in the absence of heme group, apocyt b_5 exhibits the RMSD value of core 1 and core 2 around 3.0 and 1.5 Å, respectively [25].

During the last 0.5-ns MD simulation, the C_α root mean square fluctuations (RMSF) over time of each residue presents more detailed motion of $(His)_6$-cyt b_5. An shown in Fig. 3, for heme-binding core 1, $(His)_6$-cyt b_5 displays very similar RMSF to that of cyt b_5, lower than that of apocyt b_5 in previous MD simulations due to the destabilization by heme removal from the heme-binding core 1 [25]. In case of hydrophobic core 2, $(His)_6$-cyt b_5 is found to have slightly lower RMSF value for some residues compared to cyt b_5, such as Glu21 and Glu22 in α1, and residues 90-94 in β1 and α6, due to the strong interactions with $(His)_6$-tag, as analyzed in next section. As a result, comparatively low RMSF was observed for the $(His)_6$-tag, even though it locates in the N-terminus.

Interactions of $(His)_6$-tag and cyt b_5

By inspecting the local region of $(His)_6$-tag in the modeling structure of $(His)_6$-cyt b_5, it is found that the $(His)_6$-tag interacts with the neighboring α1, α6 and β1 through salt bridges, hydrogen bonding as well as hydrophobic interactions. As shown in Fig. 4, in both structures Arg2 forms salt bridges and hydrogen bonding simultaneously with Glu21 and Asp94 that are located in α1 and α6, respectively. Glu22, another negative charged residue located in α1, interacts with the backbone N atoms, and with the neighboring Lys25 in one structure. This kind of interaction was also observed in the crystal structure of *E. Coli* YfhJ protein in which a $(His)_6$-tag is presented (PDB entry 1uj8) [30].

At the same time, hydrophobic interactions are formed among His7, Val15 and Tyr18 between His-tag and core 2 of cyt b_5, where His7 also forms a hydrogen bond with Gly11 in one structure (Fig. 4b). Note that Tyr18 located in β1 plays a crucial role in stabilizing the hydrophobic core 2 of cyt b_5 and also the entire protein structure, as illustrated recently by high temperature MD simulations [27]. The packing behavior of $(His)_6$-tag in $(His)_6$-cyt b_5 will thus extend the hydrophobic interactions from His26-Trp33-Ile87 to Tyr18-Val15-His7, resulting in stabilization of both the His-tag and the hydrophobic core 2 of cyt b_5, as reflected in Figs. 2 and 3. Three histidine residues, His5, His8 and His9, are found to locate on the same side of $(His)_6$-tag toward the solution, which likely coordinate to the Ni(II) ions during protein purification.

Effects of $(His)_6$-tag on cyt b_5

From the spatial alignment of protein polypeptide chain displayed in Fig. 1, it can be found that the $(His)_6$-tag, when attached at the N-terminus, causes little conformational disturbance to the hydrophobic core 2 of cyt b_5, the latter is responsible for stabilizing the entire protein by pre-organization of the second heme-binding core 1 [12]. Actually, what one might be interested in is the influence of $(His)_6$-tag on the heme-binding region, especially on the heme group in $(His)_6$-cyt b_5 as well as its two axial His ligands, His50 and His70. To probe such effects, we overlapped the heme group in modeling structure of $(His)_6$-cyt b_5 with the initial NMR structure as well as the crystal structure of cyt b_5, as shown in Fig. 5, including the

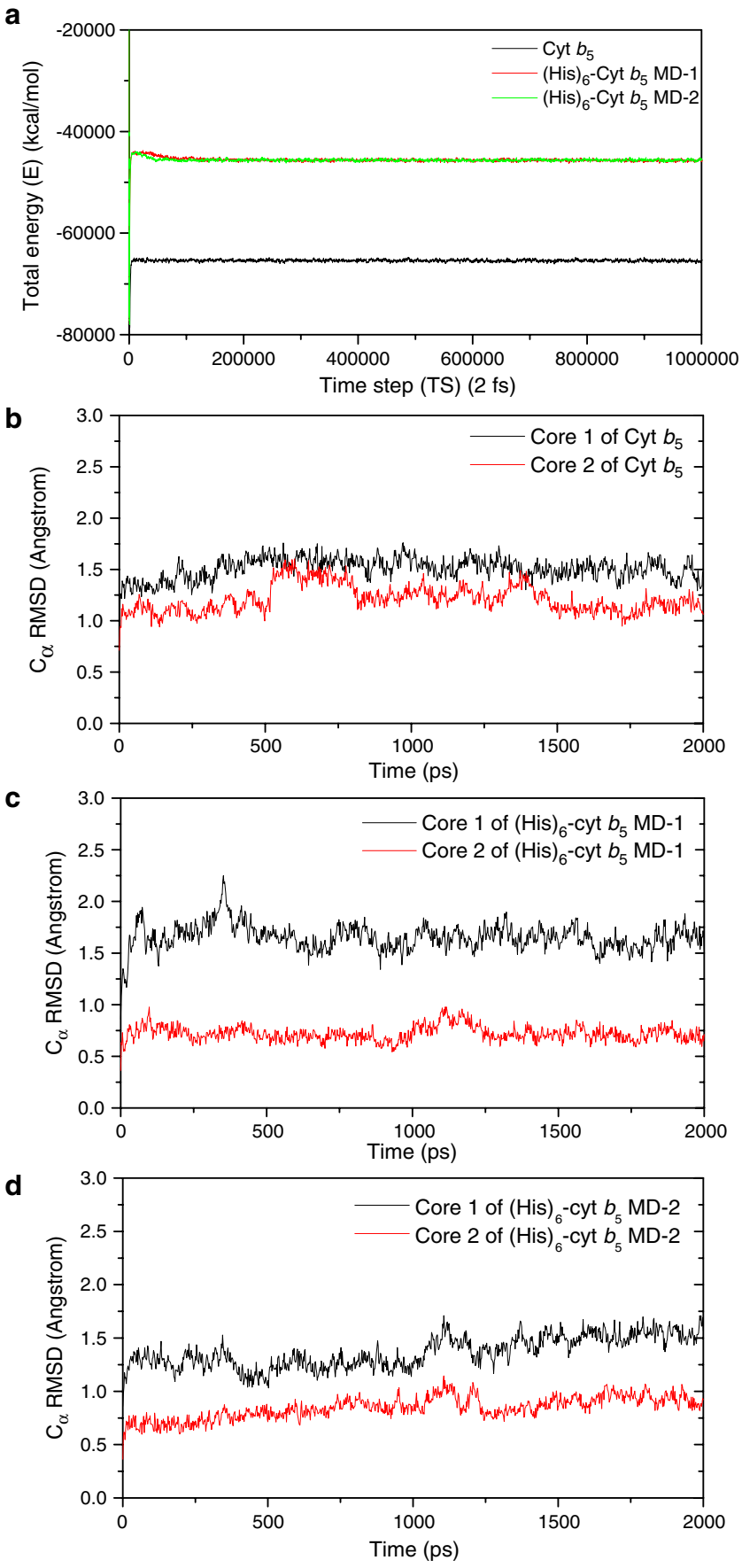

Fig. 2 (**a**) Plot of the total energy versus the time step in MD simulations of cyt b_5 and $(His)_6$-cyt b_5; (**b**) RMSD as a function of time for Core 1 and Core 2 in cyt b_5 from the initial NMR structure and in $(His)_6$-cyt b_5 from the minimization structure (**c** and **d**)

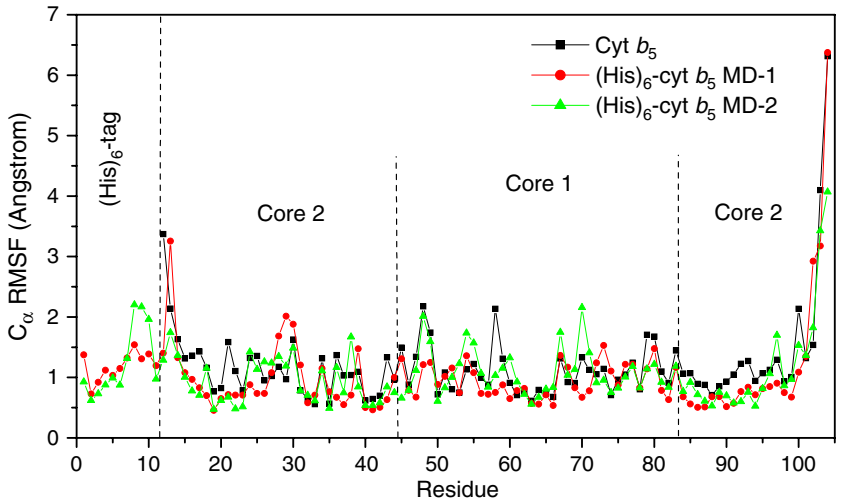

Fig. 3 Residue C_α RMSF over time during the last 0.5-ns simulation. The dashed lines separate the (His)$_6$-tag (residues 1-11), core 1 (residues 44-84) and core 2 (residues 12-43 and 85-104)

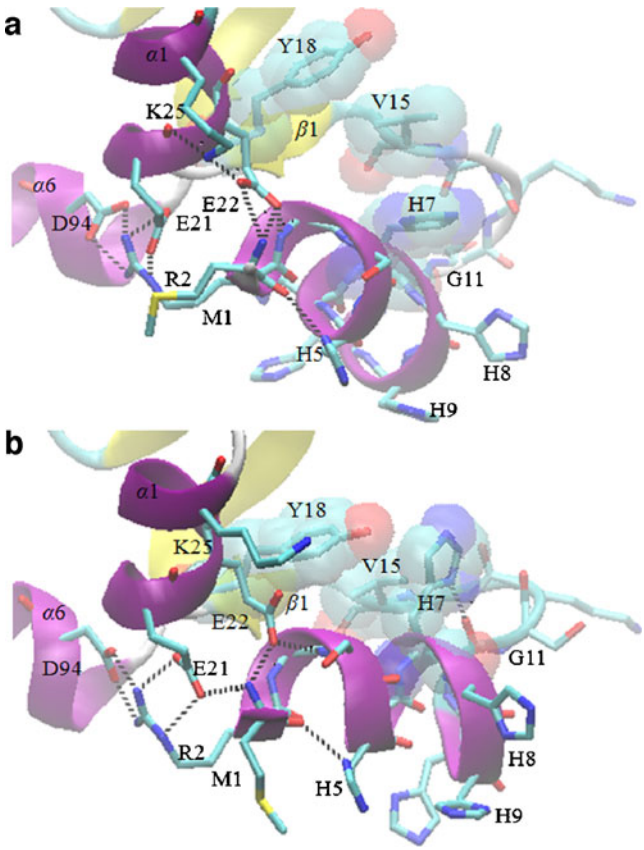

Fig. 4 Interactions between (His)$_6$-tag and the rest of protein (His)$_6$-cyt b_5 MD-1 (**a**) and (His)$_6$-cyt b_5 MD-2 (**b**). The hydrogen bonding networks are shown by dotted lines. The hydrophobic interactions between Y18, V15 and H7 are shown as VMD representation. All other residues discussed in text as well as α1, α6 and β1 are also highlighted

control simulation of isolated cyt b_5. When compared to the initial NMR structure (Fig. 5a–c), the conformation of two axial ligands is found to be similar in one (His)$_6$-cyt b_5 structure (Fig. 5c), while in the other (Fig. 5b), the two histidine imidazole rings are rotated to be nearly parallel to each other, this also happened to the simulation of cyt b_5 (Fig. 5a). However, as illustrated in Fig. 5d, e, the resultant conformation overlaps well with the crystal structure of cyt b_5 (PDB entry 1cyo). This is very interesting since although the MD simulation was performed in water solution, similar to that in NMR determination, the resultant structure is closer to the crystal structure, indicating a lower energy state can be achieved by MD simulation. The rotation of the axial histidines was also observed in previous MD simulations of other heme proteins [31–33], as well as in experimental studies of cyt b_5 and neuroglobin [34–36], which was believed to be associated with the protein function by modulating the electronic properties of the heme group.

On the other hand, comparison of the coordination distance between axial histidine ligands and heme iron shows that in both (His)$_6$-cyt b_5 structures the distance is slightly shorter than that determined by NMR or X-ray technique, while similar to the control simulation results of cyt b_5 (Table 2). This suggests that the slight change of coordination in (His)$_6$-cyt b_5 is not due to the effects of (His)$_6$-tag, but due to the MD simulation itself. The location and conformation of (His)$_6$-tag in (His)$_6$-cyt b_5 determines that it can not interact directly with the heme group. This is different from His-tagged cytochrome P450 3A5, where the histidine tag is close to the heme active site and interacts with the substrate directly [14]. Therefore, in case of core 1 in (His)$_6$-cyt b_5, the influence belongs to a distal weak interaction exerted through the hydrophobic core 2. In addition, core 2 exhibits a similar

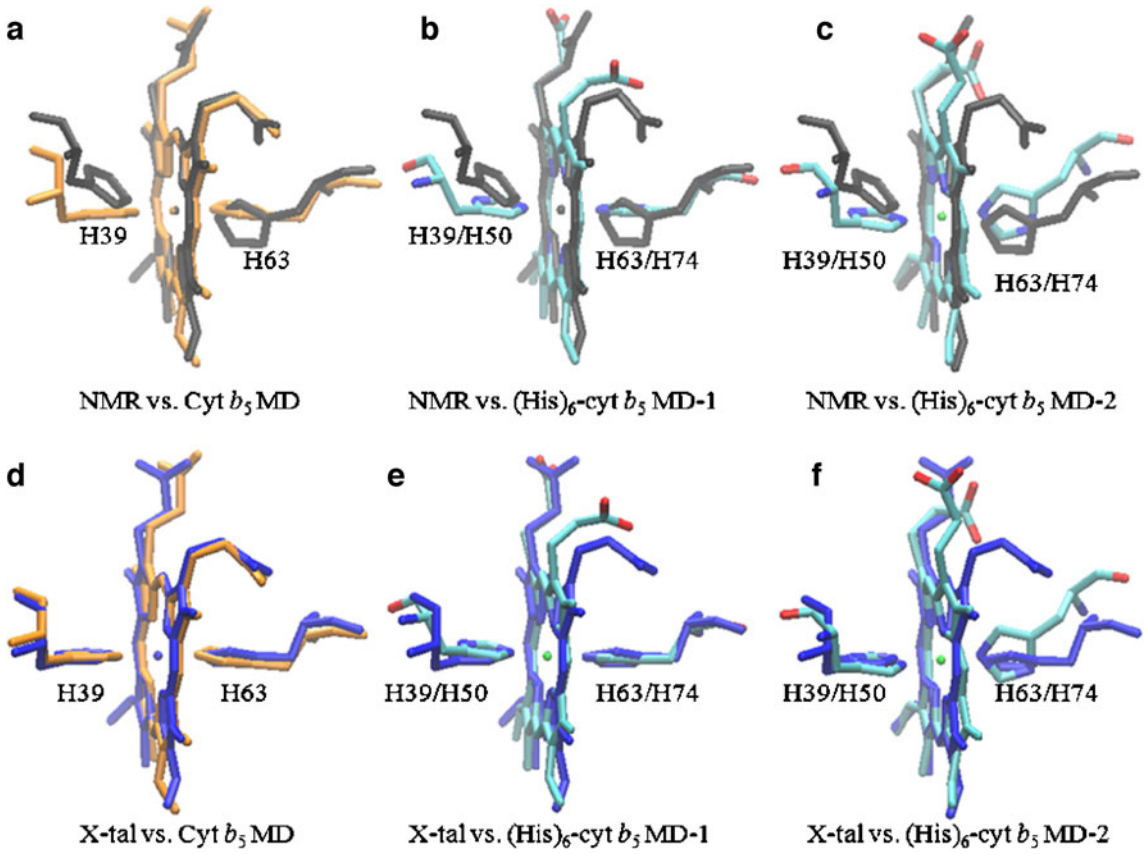

Fig. 5 Comparison of heme active sites between cyt b_5 MD result (orange), (His)$_6$-cyt b_5 (cyan) and cyt b_5 in NMR (black) (**a**, **b** and **c**) or crystal structure (blue) (**d**, **e** and **f**)

conformation in (His)$_6$-cyt b_5 compared to that in cyt b_5 (Fig. 1). These observations interpret the experimental observations that both (His)$_6$-cyt b_5 and cyt b_5 have the same UV-vis spectrum (413 nm in oxidized state, and 423, 527 and 556 nm in reduced state), as well as the similar chemical stability toward guanidine-induced unfolding (3.12 M of (His)$_6$-cyt b_5 vs. 3.18 M of cyt b_5) [8]. At the same time, the visible circular dichroism (CD) spectrum, a good conformational probe for heme proteins [37], identified a slight conformational change occurred around the heme group in (His)$_6$-cyt b_5 with respect to cyt b_5. This is also reflected in current simulations, as the rotation of heme axial ligands is observed in both simulations of (His)$_6$-cyt b_5 (Fig. 5).

Conclusions

In this study, the structure of a (His)$_6$-cyt b_5 was predicted by computer simulations. Due to the special folding module of cyt b_5, the (His)$_6$-tag introduced at the N-terminus does not interfere with the protein active site. The interactions between (His)$_6$-tag and the rest of cyt b_5 revealed in the study, both in a local position and at a long distance, provide deep insights into the experimental observations. Molecular modeling combined with MD simulations offers a convenient approach to produce a more precise image of the (His)$_6$-tag conformation, making it predictable for the consequences of introducing such an affinity tag. This can thus aid in rational design of

Table 2 Comparison of the distance between heme axial ligands and heme iron for cyt b_5 and the modeling (His)$_6$-cyt b_5 proteins (Å)

Protein	H39/H50-Fe	H63/H74-Fe
Cyt b_5 (NMR, PDB entry 1hko, model 1)	2.22	1.92
Cyt b_5 (MD simulation)	1.74	1.74
Cyt b_5 (X-tal structure, PDB entry 1cyo)	2.07	2.00
(His)$_6$-cyt b_5 (MD simulation-1)	1.72	1.74
(His)$_6$-cyt b_5 (MD simulation-2)	1.74	1.73

a His-tag protein to obtain high quantity of functional protein, and therefore its applications, especially for heme protein with alterations at heme axial His ligands that otherwise is difficult to obtain.

Acknowledgments This work was supported by the initial foundation for Ph. D. introduced in University of South China (No. 506XJQ06001). NAMD and VMD were developed by the Theoretical Biophysics Group in the Beckman Institute for Advanced Science and Technology at the University of Illinois at Urbana-Champaign, USA. We also thank Fengyun Ni at Rice University, USA, for discussion of energy minimization.

References

1. Smith MC, Furman TC, Ingolia TD, Pidgeon C (1988) J Biol Chem 263:7211–7215
2. Jenny RJ, Mann KG, Lundblad RL (2003) Protein Expr Purif 31:1–11
3. Carson D, Johnson DH, McDonald H, Brouillette C, DeLucas LJ (2007) Acta Crystallogr D 63:295–301
4. Song J, Markey JL (2007) Protein Pept Lett 14:265–268
5. Klepeis JL, Lindorff-Larsen K, Dror RO, Shaw DE (2009) Curr Opin Struct Biol 19:120–127
6. Freydank AC, Brandt W, Drager B (2008) Proteins 72:173–183
7. Lin YW, Zhao DX, Wang ZH, Huang ZX (2006) Protein Expr Purif 45:352–358
8. Lin YW (2005) Doctoral Dissertation, Fudan University, Shanghai, China, 86–106
9. Jung Y, Kwak J, Lee Y (2001) Appl Microbiol Biotechnol 55:187–191
10. Sobrado P, Goren MA, James D, Amundson CK, Fox BG (2008) Protein Expr Purif 58:229–241
11. Wang WH, Lu JX, Yao P, Xie Y, Huang ZX (2003) Protein Eng 6:1047–1054
12. Durley RC, Mathews FS (1996) Acta Crystallogr D Biol Crystallogr 52:65–76
13. Muskett FW, Kelly GP, Whitford D (1996) J Mol Biol 258:172–189
14. Emoto C, Murayama N, Wakiya S, Yamazaki H (2009) Drug Metab Lett 3:207–211
15. Guex N, Peitsch MC (1997) Electrophoresis 18:2714–2723
16. Friedrich MG, Giess F, Naumann R, Knoll W, Ataka K, Heberle J, Hrabakova J, Murgida DH, Hildebrandt P (2004) Chem Commun 21:2376–2377
17. Kalé L, Skeel R, Bhandarkar M, Brunner R, Gursoy A, Krawetz N, Phillips J, Shinozaki A, Varadarajan K, Schulten K (1999) J Comput Phys 151:283–312
18. Humphrey W, Dalke A, Schulten K (1996) J Mol Graph 14:33–38
19. Ni FY, Cai B, Ding ZC, Zheng F, Zhang MJ, Wu HM, Sun HZ, Huang ZX (2007) Proteins 68:255–266
20. Wiederstein M, Sippl MJ (2007) Nucleic Acids Res 35:W407–W410
21. Storch EM, Daggett V (1995) Biochemistry 34:9682–9693
22. Lee KH, Kuczera K (2003) Biopolymers 69:260–269
23. Cheng Q, Benson DR, Rivera M, Kuczera K (2006) Biopolymers 83:297–312
24. Storch EM, Daggett V (1996) Biochemistry 35:11596–11604
25. Lin YW, Wang ZH, Ni FY, Huang ZX (2008) Protein J 27:197–203
26. Lin YW, Ying TL, Liao LF (2009) Chin Chem Lett 20:631–634
27. Lin YW, Nie CM, Liao LF (2009) J Mol Struct Theochem 910:154–162
28. Leiros HKS, Kozielski-Stuhrmann S, Kapp U, Terradot L, Leonard GA, Mcsweeney SM (2004) J Biol Chem 279:55840–55849
29. Tajika Y, Sakai N, Tamura T, Yao M, Watanabe N, Tanaka I (2004) Proteins 57:862–865
30. Shimomura Y, Takahashi Y, Kakuta Y, Fukuyama K (2005) Proteins 60:566–569
31. Galstyan AS, Zarić SD, Knapp E (2005) J Biol Inorg Chem 10:343–354
32. Medaković V, Zarić SD (2003) Inorg Chim Acta 349:1–5
33. Zarić SD, Popović DM, Knapp E (2001) Biochemistry 40:7914–7928
34. Zhang Q, Cao C, Wang ZQ, Wang YH, Wu HM, Huang ZX (2004) Protein Sci 13:2161–2169
35. Sarma S, DiGate RJ, Goodin DB, Miller CJ, Guiles RD (1997) Biochemistry 36:5658–5668
36. Walker FA (2006) J Biol Inorg Chem 11:391–397
37. Myer YP (1970) Biochim Biophys Acta 214:94–106